Article

The Synthesis of Glycerol Carbonate from Glycerol and Carbon Dioxide over Supported CuO-Based Nanoparticle Catalyst

Jassim Mohamed Hamed Al-Kurdhani [1] and Huajun Wang [1, 2,*]

[1] Hubei Key Laboratory of Material Chemistry & Service Failure, School of Chemistry and Chemical Engineering, Huazhong University of Science and Technology, Wuhan 430074, PR China;

[2] Key Laboratory for Material Chemistry for Energy Conversion and Storage, Ministry of Education, Huazhong University of Science and Technology, Wuhan 430074, PR China

* Correspondence: wanghuajun@mail.hust.edu.cn; Tel: +86-027-87543732; Fax: +86-027-87523632

Abstract: A series of supported CuO-based nanoparticle catalysts were prepared by impregnation method and used for the synthesis of glycerol carbonate from glycerol and CO_2 in the presence of 2-cyanopyridine as a dehydrant and DMF as a solvent. The effects of supports (activated alumina, silicon dioxide, graphene oxide, graphene, and activated carbon), CuO loading amount, calcination temperature, and reaction parameters on the catalytic activity of catalyst were investigated in detail. XRD, FTIR, SEM, BET, and CO_2-TPD were used for the characterization of the prepared catalysts. It is found that CuO/Al_2O_3 shows a higher catalytic activity, which depends on the CuO loading amount and calcination temperature. The surface area and amount of basic sites of the catalyst exhibit crucial effect on the catalytic activity of CuO/Al_2O_3. Furthermore, there is a synergistic effect between the catalyst and 2-cyanopyridine that the former has higher activation ability for glycerol and the latter acts not only as a dehydrant, but also as a promoter for CO_2 activation. Recycling experiments reveal that this catalyst can be reused at least five cycles without any inactivation. Based on the experiment results and FTIR characterization, a possible reaction mechanism for the carbonylation of glycerol and CO_2 is proposed.

Keywords: glycerol; glycerol carbonate; carbon dioxide; 2-cyanopyridine; CuO/Al_2O_3

1. Introduction

Glycerol carbonate (GC) is a significant cyclic carbonate with excellent properties and broad use. GC is a nontoxic, readily biodegradable, water-soluble, not flammable (fp 165.9 °C), and viscous liquid, which can be used as a polar high boiling solvent, a surfactant component, an intermediate for many kinds of polymers. In addition, GC also can be utilized as components for gas separation membranes [1-4]. GC can be synthesized from the reaction of the biological glycerol (GL), a by-product of biodiesel, and various substances with carbonyl, such as dimethyl carbonate (DMC), or urea, or carbon dioxide. As the by-product of biodiesel manufacture, the biological GL is produced in huge amounts for the production of biodiesel is increased rapidly year by year [5-7]. Therefore, the synthesis of high value-added GC from the surplus and cheap GL has attracted more and more attentions, which is one of the main topics of biomass valorization [8-10]. Among the synthesis methods of GC, the reactions of GL with DMC or urea suffer some drawbacks, such as expensive reactant for DMC route [11-13], or generating an environmentally harmful by-product (NH_3) for urea route [14-17]. Compared with the above methods, the synthesis of GC by the carbonylation of GL with CO_2 is more interesting and its atom utilization is as high as 87%. Moreover, this reaction is regarded as a green process in which two wastes, GL, a by-product of biodiesel, and CO_2, a primary greenhouse gas, are converted into a value-added chemical, GC [18-25].

Up to now, a series of homogeneous and heterogeneous catalysts have been developed and used for the reaction of GL with CO_2. Unfortunately, however, the GL conversion and GC yield are still far from satisfactory because this reaction is severely limited by thermodynamics [20, 26-29]. Dibenedetto et al. used CeO_2/Al_2O_3 or CeO_2/Nb_2O_5 as a catalyst for the reaction of GL with CO_2 in the presence of tetraglycol dimethyl ether and found that the GL conversion only reached to 2.5% under

Preprints (www.preprints.org) | NOT PEER-REVIEWED | Posted: 25 April 2023 doi:10.20944/preprints202304.0872.v1

pressure of 5.0 MPa and reaction time of 15 h [28]. In order to break the thermodynamic limit to increase the GL conversion, the dehydrants were used in the reaction to pull out of water produced as a by-product during the reaction to shift the chemical equilibrium to product side. George et al. used the 13X zeolite as a dehydrant for the reaction of GL and CO_2 with $^nBu_2SnO$ as a catalyst and obtained GC yield of 35% (13.8 MPa, 393 K, 4 h) [21]. The acetonitrile also was used as a dehydrant for the reaction of GL and CO_2 by using Cu/La_2O_3 [19, 30], or Zn/Al/La/M(M=Li, Mg, Zr) [31], or $La_2O_2CO_3$-ZnO as a catalyst [32, 33], and the GC yield reached to 15.2%, or 18.7%, or 14.3%, respectively. Recently, He et al. used 2-cyanopyridine as a dehydrant and CeO_2 as a catalyst for the reaction of GL and CO_2. Although a higher GC yield of 78.9% was obtained in this process, the catalyst amount was too higher (187 wt% based on GL weight) to the industrial production of GC [18]. These results indicate that the GL conversion and GC yield increase assuredly due to introduction of the dehydrant for the reaction of GL and CO_2. Compared with acetonitrile and 13X zeolite, 2-cyanopyridine is more suitable for the reaction of GL with CO_2 because a higher GC selectivity and a fewer side reaction would be obtained; moreover, Zhao et al. found that 2-cyanopridine not only acts as the dehydrant, but also actives the carbonyl bond of CO_2 [35]. However, in spite of these progresses, the GC yield is still not enough high for the industrial production and it is also urgently requisite to develop new more effective catalyst for the synthesis of GC from GL and CO_2.

The supported CuO-based nanocatalysts were used in various applications such as the low-temperature water-gas shift reaction, oxidation of various amounts of SO_2, oxidation of volatile organic compounds (VOCs), oxidation of methane, epoxidation of alkenes through oxygen activation, catalyst-sorbent suitable for simultaneous SO_2 and NOx removal from flue gases, etc [36-40]. However, to the best of our knowledge, there are few reports on the synthesis of GC from GL and CO_2 by means of using supported CuO-based nanoparticle as a catalyst. In the present work, a series of CuO-based catalysts were prepared and used for the synthesis of GC by the carbonylation of GL and CO_2 in the presence of 2-cyanopyridine as a dehydrant and DMF as a solvent (scheme 1). XRD, FTIR, SEM, BET method, and CO_2-TPD were used to scrutinize physicochemical properties of the prepared catalysts. The effects of supports (activated alumina, silicon dioxide, graphene oxide, graphene, and activated carbone), CuO loading amount, calcination temperature, and reaction parameters (CO_2 pressure, reaction temperature, time, and catalyst amount) on the catalytic activity of catalyst were investigated in detail. Finally, based on the experiment results and FTIR characterization, a possible reaction mechanism for the carbonylation of GL and CO_2 was proposed.

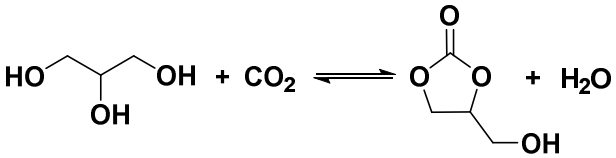

Scheme 1 The synthesis of GC from the reaction of GL with CO_2

2. Result and discussion

2.1. Effect of supports

The catalytic activities of supported CuO-based catalysts with different supports, such as graphene oxide (GO), activated carbone (AC), SiO_2, graphene (GE), and Al_2O_3 for the synthesis of GC from GL and CO_2 are given in Table 1. It is found that among these catalysts, CuO/AC(30%, 500) shows the lowest catalytic activity with GL conversion of 21.4% and GC yield of 8.9%. In contrast, the CuO/Al_2O_3(30%, 500) gives the highest catalytic activity and GL conversion and GC yield reach to 37.8% and 15.0%, respectively, over CuO/Al_2O_3(30%, 500). Although CuO/GO(30%, 500), CuO/GE(30%, 500), and CuO/SiO_2(30%, 500) show higher GL conversion than CuO/Al_2O_3(30%, 500), CuO/Al_2O_3 catalyst possesses higher GC yield and GC selectivity. So, CuO/Al_2O_3 catalyst with activated Al_2O_3 as the support is suitable for the synthesis of GC from the reaction of GL with CO_2. In the next section, the catalytic activities of CuO/Al_2O_3 with different CuO loading amounts and calcination temperatures were investigated.

Preprints (www.preprints.org) | NOT PEER-REVIEWED | Posted: 25 April 2023 doi:10.20944/preprints202304.0872.v1

Table 1. The catalytic activities of supported CuO-based catalysts with different supports for the synthesis of GC from GL and CO_2. [a]

Catalyst	T_{cal}(°C)	W_{CuO}(wt%)	X_{GL}(%)	Y_{GC}(%)	S_{GC}(%)
CuO/GO(30%, 500)	500	30	49.0	14.6	29.7
CuO/AC(30%, 500)	500	30	21.4	8.9	41.4
CuO/SiO_2(30%, 500)	500	30	38.2	10.1	26.5
CuO/GE(30%, 500)	500	30	49.0	13.4	27.3
CuO/Al_2O_3(30%, 500)	500	30	37.8	15.0	39.8

[a] reaction condition: GL: 2.30 g; Cat: 1.0 g, CO_2 initial pressure: 4.0 MPa; reaction temperature: 150 °C; reaction time: 5 h; 2-cyanopyridine: 6.32 g; DMF: 19.0 g.

2.2. Effect of CuO loading amount and calcination temperature

The CuO/Al_2O_3 catalysts with different CuO loading amounts were also prepared by impregnation method and then used for the synthesis of GC from GL and CO_2. It is found that the CuO loading amount has remarkable effect on the catalytic activity of the CuO/Al_2O_3 catalyst (Table 2). As the CuO loading amount are increased from 5 wt% to 30 wt%, the GL conversion and GC yield increase from 14.6% and 2.8% to 37.8% and 15.0%, respectively. When the CuO loading amount is further increased from 30% to 40%, though the GL conversion increases from 37.8% to 51.6%, the GC yield increases slightly from 15.0% to 15.3% and the GC selectivity decreases from 39.8% to 29.7%. It indicates that CuO loading amount of 30% should be suitable for GC synthesis from the reaction of GL and CO_2.

Table 2 also demonstrates the effect of calcination temperature on the catalytic activity of CuO/Al_2O_3 catalyst. It is found that with the increase of the calcination temperature from 400 °C to 800 °C, the GL conversion decreases from 58.0% to 33.5% while the GC yield firstly increases from 15.1% to 17.5% and then decreases to 14.2%. Among these catalysts, CuO/Al_2O_3(30%, 700) possesses the highest GC yield of 17.5% and GC selectivity of 42.4%.

Table 2. The catalytic activity of CuO/Al_2O_3 catalysts with different CuO loading amounts and calcination temperatures for the synthesis of GC from GL and CO_2.[a]

Catalyst	T_{cal}(°C)	W_{CuO}(wt%)	X_{GL}(%)	Y_{GC}(%)	S_{GC}(%)
CuO/Al_2O_3(5%, 500)	500	5	14.6	2.8	19.2
CuO/Al_2O_3(10%, 500)	500	10	17.9	6.0	33.5
CuO/Al_2O_3(20%, 500)	500	20	29.4	10.0	34.1
CuO/Al_2O_3(30%, 500)	500	30	37.8	15.0	39.8
CuO/Al_2O_3(40%, 500)	500	40	51.6	15.3	29.7
CuO/Al_2O_3(30%, 400)	400	30	58.0	15.1	26.0
CuO/Al_2O_3(30%, 600)	600	30	44.0	13.6	30.9
CuO/Al_2O_3(30%, 700)	700	30	41.3	17.5	42.4
CuO/Al_2O_3(30%, 800)	800	30	33.5	14.2	42.4

[a] Reaction condition: GL: 2.30 g; Cat: 1.0 g; CO_2 initial pressure: 4.0 MPa; reaction temperature: 150 °C; reaction time: 5 h; 2-cyanopyridine: 6.32 g; DMF: 19.0 g.

Preprints (www.preprints.org) | NOT PEER-REVIEWED | Posted: 25 April 2023 doi:10.20944/preprints202304.0872.v1

2.3. Characterization

2.3.1. XRD

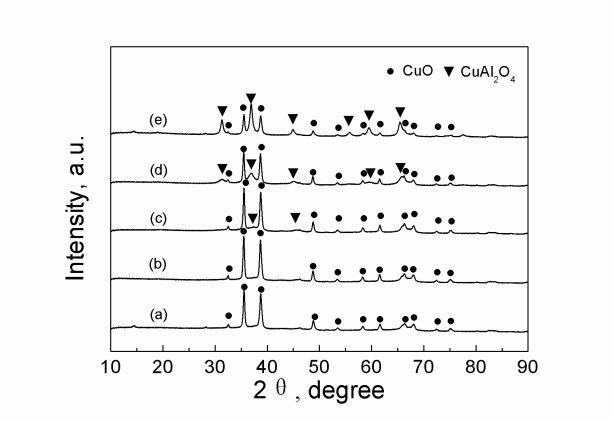

Figure 1. X-ray diffraction patterns of CuO/Al_2O_3 nanoparticle catalysts calcined at different temperatures: (a) CuO/Al_2O_3(30%, 400), (b) CuO/Al_2O_3(30%, 500), (c) CuO/Al_2O_3(30%, 600), (d) CuO/Al_2O_3(30%, 700), (e) CuO/Al_2O_3(30%, 800).

Figure 1 shows the XRD patterns of CuO/Al_2O_3 nanoparticle catalysts calcined at different temperatures. It is found that when calcination temperature is less than 700 °C, the main phase of the samples CuO/Al_2O_3(30%, 400~600) is monoclinic CuO (at 2θ = 32.5°, 35.5°, 38.7°, 46.2°, 48.7°, 53.3°, 58.3°, 61.5°, 66.2°, 72.3°, 75.2°). Meanwhile, the diffraction intensity of CuO phase slightly increases with the calcination temperature by comparing the peak at 35.5°. It means that the degree of crystallinity of the sample increases slightly with the calcination temperature. In addition, at the calcination temperature of 600 °C, a new phase, cubic $CuAl_2O_4$ (at 2θ = 31.4°, 36.9°, 44.85°, 55.7°, 59.4°, 65.4°) is observed, which must be formed by the interaction of $Cu(NO_3)_2$ with supporter Al_2O_3, indicating that Cu^{2+} is successfully loaded onto Al_2O_3 skeleton [41,42]. As the calcination temperature further increases from 600 °C to 800 °C, the diffraction intensity of CuO phase becomes weaker. On the contrary, the diffraction intensity of $CuAl_2O_4$ phase becomes stronger, implying the fact that the content of CuO phase decreases while content of $CuAl_2O_4$ phase increases with the rise of calcination temperature (Figure 1 (c-e)). It indicates that a higher calcination temperature is benefit for the interaction of $Cu(NO_3)_2$ with supporter Al_2O_3 to produce more $CuAl_2O_4$ species. For all samples, no peak related to Al_2O_3 phase is found. It is expected that the calcined Al_2O_3 may be presented in the form of η-alumina with low crystallinity.

The mean grain size of CuO in the CuO/Al_2O_3(30%, 400~800) catalysts is calculated by the Scherrer equation based on the reflection peak of CuO at 35.5° and the results are 25.3 nm, 26.6 nm, 26.9 nm, 29.6 nm, and 26.0 nm for CuO/Al_2O_3(30%, 400~800), respectively [42]. It can be seen that the mean grain size of CuO increases with the calcination temperature (except sample at 800 °C), indicating that the higher temperature is favorable for the growth of the CuO particles. However, the CuO/Al_2O_3(30%, 800) has a smaller CuO grain size of 26.0 nm and the reason may be that the generation of the $CuAl_2O_4$ phase restrains the growth of the CuO particle.

Preprints (www.preprints.org) | NOT PEER-REVIEWED | Posted: 25 April 2023 doi:10.20944/preprints202304.0872.v1

2.3.2. FTIR

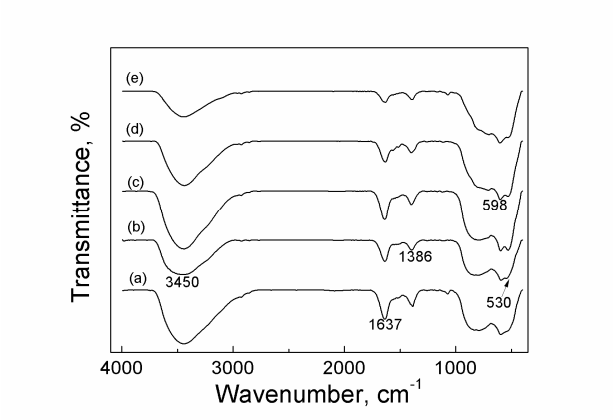

Figure 2. FTIR spectra of CuO/Al_2O_3 nanoparticle catalysts calcined at different temperatures: (a) CuO/Al_2O_3(30%, 400), (b) CuO/Al_2O_3(30%, 500), (c) CuO/Al_2O_3(30%, 600), (d) CuO/Al_2O_3(30%, 700), (e) CuO/Al_2O_3(30%, 800)

Figure 2 shows the FT-IR spectra of the CuO/Al_2O_3 nanoparticles. For all the fresh CuO/Al_2O_3 catalysts, the weak peaks at 1637 cm^{-1} and 1386 cm^{-1} and the wide band at 3000~3700 cm^{-1} are assigned to the bending and stretching vibration of –OH of the adsorbed water molecule [43]. The intensities of these peaks decrease gradually with the increase of the calcination temperature, indicating that the water content in the nanoparticle decreases with the rise of the calcination temperature. The peaks at 530 cm^{-1} and 598 cm^{-1} are attributable to the stretching vibration of Cu-O [44]. The FT-IR result suggests that the formation of the CuO compound is obtained after calcination process, which is consistent with XRD result.

2.3.3. SEM

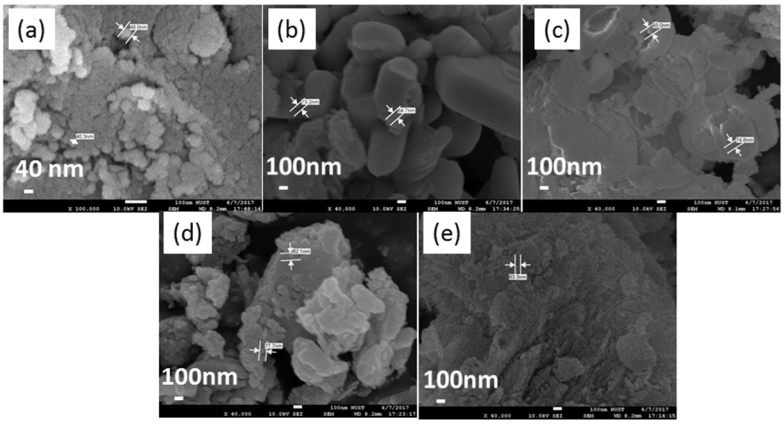

Figure 3. SEM images of CuO/Al_2O_3 nanoparticle catalysts calcined at different temperatures: (a) CuO/Al_2O_3 (30%, 400), (b) CuO/Al_2O_3 (30%, 500), (c) CuO/Al_2O_3 (30%, 600), (d) CuO/Al_2O_3 (30%, 700), (e) CuO/Al_2O_3 (30%, 800)

Figure 3 shows the SEM images of the CuO/Al_2O_3 nanoparticle catalysts with different temperatures. It is found that the calcination temperature has remarkable effect on the morphology and size of the nanoparticle. The CuO/Al_2O_3 (30%, 400) nanoparticle is spherical and its diameter is about 50 nm. In this sample, the edge of nanoparticle is unsmooth, meaning that some particles may be secondary particle. For CuO/Al_2O_3 (30%, 500) sample, the particle displays polyhedron or sheet structure with large diameter, which should be formed by the agglomeration of minicrystals. For the CuO/Al_2O_3 (30%, 600), the particles are seriously agglomerated to form blocky structure while for

Preprints (www.preprints.org) | NOT PEER-REVIEWED | Posted: 25 April 2023 doi:10.20944/preprints202304.0872.v1

CuO/Al_2O_3 (30%, 700) sample, the nanoparticles are agglomerated to form large nutty structure. In addition, for the CuO/Al_2O_3 (30%, 800) sample, the nanoparticles are agglomerated to form spongy structure. These results indicate that at higher calcination temperature, the thermal diffusion behavior of the catalyst components takes place to form particles with various shapes, which may have an obvious effect on the catalytic activity of the nanoparticle by affecting the adsorption, desorption, and surface reaction process of the reaction components. For these samples, compared with the nanoparticles with blocky and spongy structure, the samples with granular structure may be more favorable to the synthesis of GC for the CuO/Al_2O_3 (30%, 400, 500, 700) show higher GC yields than CuO/Al_2O_3 (30%, 600) and CuO/Al_2O_3 (30%, 800) (see Table 2).

2.3.4. BET

The N_2 adsorption-desorption isotherms of CuO/Al_2O_3(30%, 600~800) are showed in Figure 4. The related BET specific surface areas, total pore volumes, and average pore diameters are listed in Table 3. All the catalysts exhibited the type IV isotherms with the type III hysteresis loops in terms of IUPAC classification [29]. The result indicates that the prepared CuO/Al_2O_3 belongs to the mesoporous nanoparticle. With the increase of calcination temperature from 600 °C to 700 °C, although the mean grain size of CuO increases from 26.9 nm to 29.6 nm (see XRD results), the specific surface area remarkably increases from 111.29 m^2/g to 170.52 m^2/g while the total pore volume slightly increases from 0.269 cm^3/g to 0.277 cm^3/g (in Table 3). The increasing in the specific surface area may be related to the morphology of sample nanoparticle. The loosened nutty structure constituted by the granules for CuO/Al_2O_3(30%, 700) may be more favorable to generate large surface area than the pyknotic blocky structure for CuO(30%, 600) (Figure 3). When the calcination temperature increases further to 800 °C, the surface area and the total pore volume of CuO/Al_2O_3(30%, 800) decrease to 92.7 m^2/g and 0.240 cm^3/g, respectively. Among these catalysts, the CuO/Al_2O_3(30%, 700) shows the largest surface area and total pore volume, which may cause the exposure of more active sites and leads to a higher catalytic activity. Table 2 shows that among these catalysts, CuO/Al_2O_3(30%, 700) has the highest GC yield, meaning that the catalytic activity may correlate to the surface area and total pore volume. However, although the surface area and the total pore volume of the CuO/Al_2O_3(30%, 800) are lower than that of CuO/Al_2O_3(30%, 600), the GC yield over CuO/Al_2O_3(30%, 800) is slightly higher than that over CuO/Al_2O_3(30%, 600) (see Table 2), which indicates that the catalytic activity does not only correlated to the surface area of the catalyst.

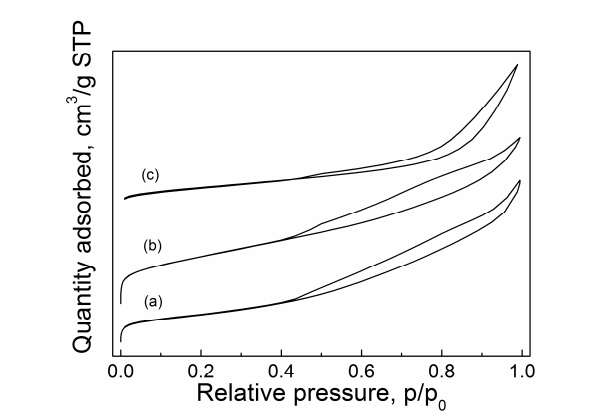

Figure 4. N_2 adsorption-desorption isotherms of CuO/Al_2O_3 nanoparticle catalysts calcined at different temperatures: (a) CuO/Al_2O_3(30%, 600), (b) CuO/Al_2O_3(30%, 700), and (c) CuO/Al_2O_3(30%, 800)

Preprints (www.preprints.org) | NOT PEER-REVIEWED | Posted: 25 April 2023 doi:10.20944/preprints202304.0872.v1

Table 3. The BET surface area, total pore volume, and average pore diameter of CuO/Al_2O_3(30%, 600-800) catalysts

Catlysts	S_{BET} (m^2/g)	Total pore volume (cm^3/g)	Average pore diameter (nm)	Basic site amount (umol/g)			
				< 200 °C	200~400 °C	>400 °C	total
CuO/Al_2O_3(30%,600)	111.29	0.269	7.98	171.18(0.19) [a]	367.13(0.42)	337.15(0.39)	875.45
CuO/Al_2O_3(30%,700)	170.52	0.277	6.65	193.86(0.18)	184.90(0.17)	703.66(0.65)	1082.42
CuO/Al_2O_3(30%,800)	92.70	0.240	11.42	4.91(0.02)	90.16(0.27)	233.86(0.71)	328.93

[a] the number in bracket is the ratio of the each basic sites amount to the total basic sites number.

2.3.5. CO_2-TPD

Figure 5 shows the CO_2-TPD profiles of the CuO/Al_2O_3(30%, 600~800) catalysts. The CO_2 desorption peaks can be roughly divided into three regions: the weak (100 ~ 200 °C), moderate (200~400 °C), and strong (> 400 °C) basic sites. The basic sites amounts can be estimated by integrating the peak area and the results are listed in Table 3. It can be found that with increase of calcination temperature from 600 °C to 700 °C, the total basic sites amount and strong basic sites amount increase from 875.45 umol/g and 337.15 umol/g to 1082.42 umol/g and 703.66 umol/g, respectively, while the moderate basic sites amount decreases from 367.13 umol/g to 184.90 umol/g. When the calcination temperature further increases to 800 °C, the total basic sites amount, the strong basic sites amount, and the moderate sites amount decrease to 328.93 umol/g, 233.86 umol/g, and 90.16 umol/g, respectively. For these samples, the more surface area a catalyst possesses, the more basic sites it has and vice versa. Among these catalysts, CuO/Al_2O_3(30%, 700) possesses the highest surface area, so it has the most amount of total basic sites. On the contrary, CuO/Al_2O_3(30%, 800) has the least surface area, thereby it possesses the least amount of total basic sites. In addition, the CuO/Al_2O_3(30%, 700) has more amount of strong basic sites and lesser amount of moderate basic sites than CuO/Al_2O_3(30%, 600) may be ascribed to that the former possesses the more $CuAl_2O_4$ species and lesser CuO phase (see Figure 1 (d, e)). It meaning that $CuAl_2O_4$ phase may have a higher strong basic site and CuO phase may contain a higher amount of moderate basic sites. By the same token, though the CuO/Al_2O_3(30%, 800) possesses the least amount of total basic sites, its ratio of amount of strong basic sites is 0.71 which is the highest among these samples for the content of $CuAl_2O_4$ phase is highest (see Figure 1 (c~e)).

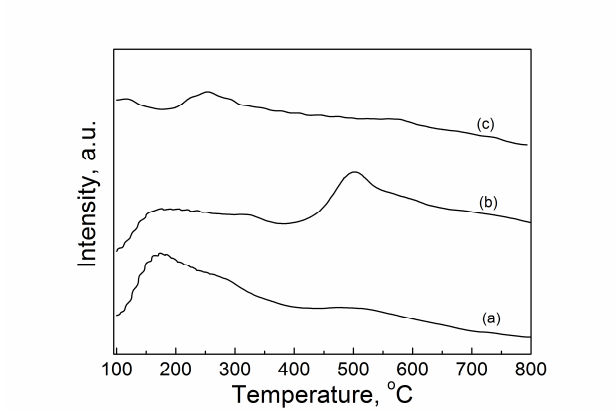

Figure 5. CO_2-TPD profiles of CuO/Al_2O_3 nanoparticle catalysts calcined at different temperatures: (a) CuO/Al_2O_3(30%, 600), (b) CuO/Al_2O_3(30%, 700), (c) CuO/Al_2O_3(30%, 800)

The previous research results indicated that the basic sites amount on the catalyst surface is very important for the activation of CO_2 in the synthesis of dimethyl carbonate from methanol and CO_2 [45]. Therefore, the CuO/Al_2O_3(30%, 700) exhibits the higher GC yield may be attributed to a higher

Preprints (www.preprints.org) | NOT PEER-REVIEWED | Posted: 25 April 2023 doi:10.20944/preprints202304.0872.v1

total basic sites amount. Furthermore, although the total basic sites amount of CuO/Al_2O_3(30%, 800) is smaller, this catalyst shows higher GC yield, which may be ascribed to the higher ratio of strong basic sites amount. The $CuAl_2O_4$ phase with more strong basic sites may have a strong ability to extract a hydrogen atom from the hydroxyl (–OH) of GL to activate GL [46]. In addition, Wei et al, found that the moderate basic sites are beneficial to active CO_2 [31], thereby, the catalysts with more CuO phase with a more moderate basic sites amount, such as CuO/Al_2O_3(30%, 400) and CuO/Al_2O_3(30%, 500) (see Figure 1), also exhibit a higher GC yield. The above results indicate that a large surface area and higher amount of strong basic sites and moderate basic sites are crucial for the reaction of GL with CO_2.

2.4. Effect of reaction condition

2.4.1. Effect of reaction temperature

Figure 6 shows the effect of reaction temperature on the catalytic activity of CuO/Al_2O_3(30%, 700) for the reaction of GL with CO_2. With the increase of reaction temperature from 100 °C to 150 °C, the GL conversion and GC yield increase from 15.0% and 2.7% to 41.3% and 17.5%, respectively, while the GC selectivity increases from 18.1% to 42.3%. With the further increase of reaction temperature to 160 °C, the yield and selectivity of GC almost keep constant. So, the best reaction temperature is 150 °C.

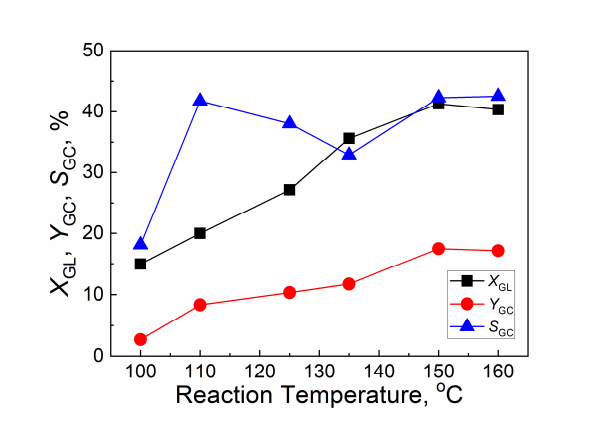

Figure 6. The effect of reaction temperature on the catalytic activity of CuO/Al_2O_3(30%, 700) for the reaction of GL with CO_2 (Reaction condition: GL: 2.30 g; Cat: 1.0 g; CO_2 initial pressure: 4.0 MPa; reaction time: 5 h; 2-cyanopyridine: 6.32 g; DMF: 19.0 g.)

2.4.2. Effect of CO_2 initial pressure

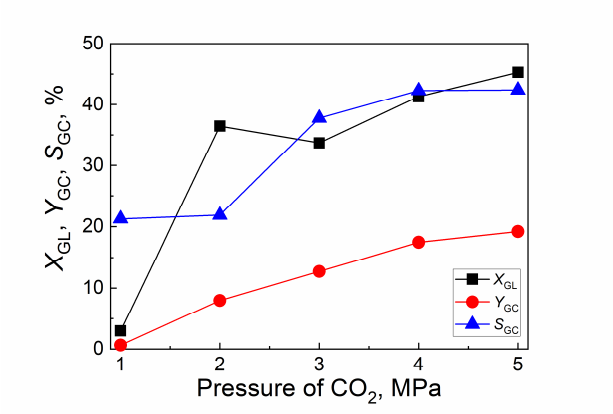

Figure 7. The effect of CO_2 initial pressure on the catalytic activity of CuO/Al_2O_3(30%, 700) for the reaction of GL with CO_2 (Reaction condition: GL: 2.30 g; Cat: 1.0 g; reaction temperature: 150 °C; reaction time: 5 h; 2-cyanopyridine: 6.32 g; DMF: 19.0 g.)

Preprints (www.preprints.org) | NOT PEER-REVIEWED | Posted: 25 April 2023 doi:10.20944/preprints202304.0872.v1

Figure 7 illustrates the effect of CO_2 initial pressure on the catalytic activity of CuO/Al_2O_3(30%, 700) catalyst for the reaction of GL with CO_2. As CO_2 initial pressure increases from 1.0 MPa to 4.0 MPa, the GL conversion increases from 3.0% to 41.3% while the GC yield and GC selectivity increase from 0.6% and 21.3% to 17.5% and 42.3%, respectively. With the further increase of CO_2 pressure to 5.0 MPa, the GL conversion, GC yield, and GC selectivity slightly increase. So, the suitable CO_2 initial pressure is 4.0~5.0 MPa.

2.4.3. Effect of reaction time

Figure 8 shows the effect of reaction time on the catalytic activity of CuO/Al_2O_3(30%, 700) for the reaction of GL with CO_2. As the reaction time increases from 1 h to 5 h, the GL conversion increases from 8.8% to 41.3%, while the GC yield and GC selectivity continually increase from 0.7% and 7.4% to 17.5% and 42.3%, respectively. With the further increase of reaction time to 6 h, the yield and selectivity of GC are slightly decreased. So, the suitable reaction time is 5 h.

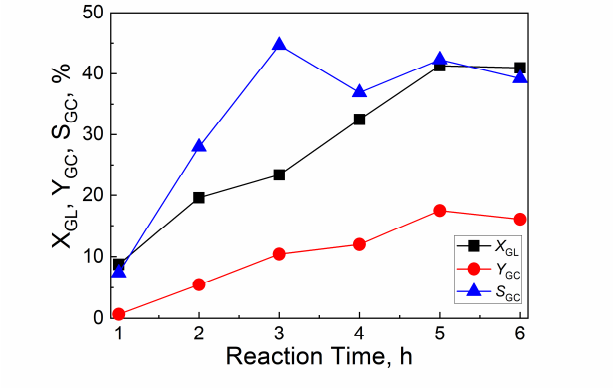

Figure 8. The effect of reaction time on the catalytic activity of CuO/Al_2O_3(30%, 700) for the reaction of GL with CO_2 (Reaction condition: GL: 2.30 g; Cat: 1.0 g; CO_2 initial pressure: 4.0 MPa; reaction temperature: 150 °C; 2-cyanopyridine: 6.32 g; DMF: 19.0 g.)

2.4.4. Effect of weight of catalyst

The effect of weight of catalyst on the catalytic activity of CuO/Al_2O_3(30%, 700) is illustrated in Figure 9. As the weight of catalyst increases from 0.25 g to 1.0 g, the GL conversion decreases from 31.7% to 41.3%, while GLC yield and GLC selectivity increase from 7.2% and 22.9% to 17.5% and 42.3%, respectively. With the further increase of weight of catalyst, the GL conversion, GLC yield, and GLC selectivity decrease slightly. So, the suitable weight of catalyst is 1.0 g.

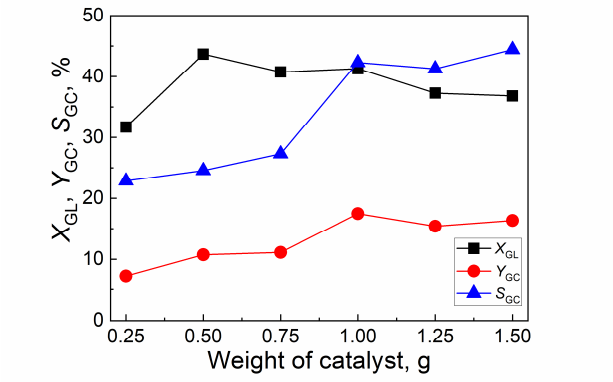

Figure 9. The effect of weight of catalyst on the catalytic activity of CuO/Al_2O_3(30%, 700) for the reaction of GL with CO_2 (Reaction condition: GL: 2.30 g; CO_2 initial pressure: 4.0 MPa; reaction temperature: 150 °C; reaction time: 5 h; 2-cyanopyridine: 6.32 g; DMF: 19.0 g.)

Preprints (www.preprints.org) | NOT PEER-REVIEWED | Posted: 25 April 2023 doi:10.20944/preprints202304.0872.v1

2.5. Stability of CuO/Al₂O₃(30%, 700) catalyst

The recycling experiments were also carried out to scrutinize the stability of CuO/Al₂O₃(30%, 700) catalyst. After the reaction, the catalyst was separated by centrifugation, washed with methanol three times and then reused for the next run under the same condition. As shown in Figure 10, at the fifth recycle, the GL conversion and GC yield still can reach 43.4% and 17.4%, respectively, over the recovered CuO/Al₂O₃(30%, 700) catalyst. These results indicate that the CuO/Al₂O₃(30%, 700) has strong stability in the activity during the reaction process.

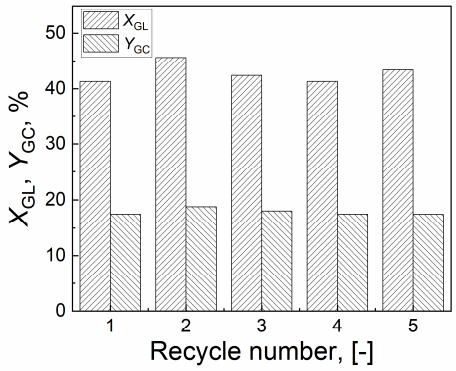

Figure 10. The stability of CuO/Al₂O₃(30%, 700) catalyst on the reaction of GL with CO_2 (Reaction condition: GL: 2.30 g; Cat: 1.0 g; CO_2 initial pressure: 4.0 MPa; reaction temperature: 150 °C; reaction time: 5 h; 2-cyanopyridine: 6.32 g; DMF: 19.0 g.)

2.6. Proposed reaction mechanism

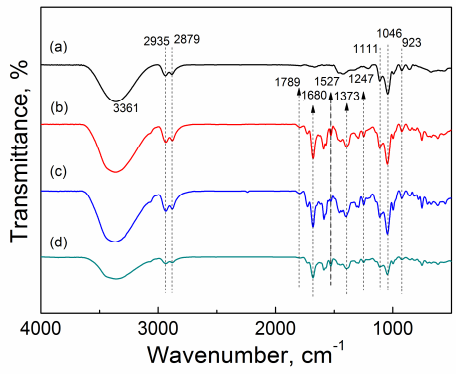

Figure 11. FT-IR spectra of reaction mixture with different reaction time: (a) 0 min; (b) 60 min; (c) 120 min; (d) 180 min.

In order to clearly understand the reaction mechanism of carbonylation of GL with CO_2 over CuO/Al₂O₃ in the presence of 2-cyanopyridine as a dehydrant with DMF as a solvent, the FT-IR spectra were used to characterize the reaction mixture with different reaction time. As shown in Figure 11 (a), the peaks at 3361 cm^{-1}, 2935 cm^{-1}, 2879 cm^{-1}, and 923 cm^{-1} are attributed to the vibration of –OH of GL molecular [47] and the bands at 1046 cm^{-1} and 1111 cm^{-1} to the C-O stretching of GL [31], whose strengths decrease with the increase of reaction time (Figure 11 (b, c, d)), indicating that the amount of GL gradually decreases in the reaction mixture due to the reaction consumption. Furthermore, some new bands centered at 1789 cm^{-1}, 1680 cm^{-1}, 1527 cm^{-1}, 1373 cm^{-1}, and 1247 cm^{-1} appear for mixture at 60 min, 120 min, and 180 min, compared with sample at 0 min. The peak at 1789 cm^{-1} is ascribed to the stretching vibration of C=O of GC [47]. The peak at 1373 cm^{-1} is assigned to the C-N bond in the ring and the peak at 1527 cm^{-1} is attributed to the C=N bond (N in C≡N).

Preprints (www.preprints.org) | NOT PEER-REVIEWED | Posted: 25 April 2023 doi:10.20944/preprints202304.0872.v1

Meanwhile, the band at 1247 cm^{-1} is ascribed to the new C-N bonds formed from the interaction between the cyano group of 2-cyanopyridine and CO_2 while the band at 1680 cm^{-1} is assigned to the C=O bond [35]. These peaks mean that an intermediate species may be formed by the interaction of CO_2 with 2-cyanopyridine molecule (Scheme 2), resulting in activation of CO_2. These results are in accordance with the reports by Zhao et al., in which a five-membered ring intermediate was also proved to be formed from reaction of 2-cyanopyridine with CO_2 for the activation of CO_2 [35]. Meanwhile, He et al. found that when DMF was mixed with GL and 2-cyanopyridine and then treated with CO_2, the five membered ring intermediate was not produced, meaning DMF as a solvent could weaken the interaction between 2-cyanopyridine and CO_2 and therefore, CO_2 could not be activated in the mixture of GL + 2-cyanopyridine + DMF [22]. However, the results in the present work indicate that though there is DMF in the mixture, CO_2 can still be activated by 2-cyanopyride.

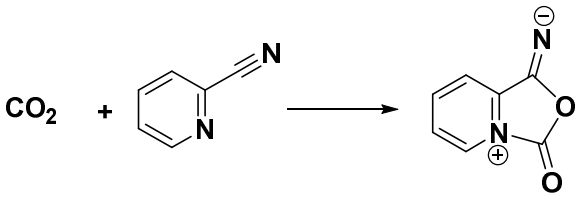

Scheme 2. The interaction of CO_2 with 2-cyanopyridine to form an intermediate.

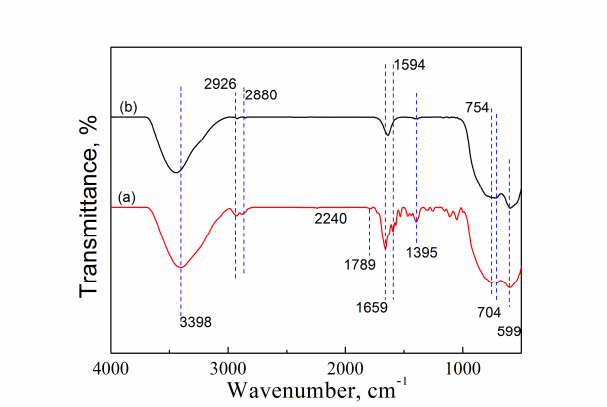

Figure 12. FT-IR spectra of (a) recovered CuO/Al_2O_3(30%, 700) and (b) fresh CuO/Al_2O_3(30%, 700).

The recovered CuO/Al_2O_3(30%, 700) catalyst was also characterized by FT-IR as well as the fresh catalyst and the results are illustrated in Figure 12. Compared with the fresh catalyst, the recovered CuO/Al_2O_3(30%, 700) exhibits several new peaks in FT-IR spectra (Figure 12 (a)). The band at 1789 cm^{-1} is attributed to GC while the peak centered at 754 cm^{-1} is assigned to picolinamide, the product of hydration reaction of 2-cyanopyridine and water. The band at 2926 cm^{-1} and 2880 cm^{-1} become large and shift to high frequency, indicating that GL molecular is adsorbed on the active sites of catalyst. The peak at 1594 cm^{-1} may be an evidence for the formation of $Cu(C_3O_3H_6)$ from the interaction of GL with CuO/Al_2O_3(30%, 700) catalyst [23]. Furthermore, the little peak at 2240 cm^{-1} is ascribed to 2-cyanopyridine while the peak at 1395 cm^{-1} is belonged to CO_2 [22]. These results indicate that GL, 2-cyanopyridine, and CO_2 can be activated on the CuO/Al_2O_3 catalyst. However, the activated CO_2 molecule may prefer to interact with 2-cyanopyridine to form a more highly active intermediate rather than to react directly with GL [35]. It means that CuO/Al_2O_3(30%, 700) catalyst can accelerate the interaction of CO_2 and 2-cyanopyridine, which may be the reason why the active intermediate can be generated in the presence of DMF.

Based on these experimental and characterization results, a possible reaction route for the synthesis of GC from GL and CO_2 is proposed and shown in Scheme 3. During the reaction, firstly, the primary O-H bond of GL is activated by adsorption on the strong basic sites of CuO/Al_2O_3 catalyst. Afterwards, the second O-H bond of GL is also activated by interaction with CuO/Al_2O_3 to

Preprints (www.preprints.org) | NOT PEER-REVIEWED | Posted: 25 April 2023 doi:10.20944/preprints202304.0872.v1

form the Cu($C_3O_3H_6$) while the CO_2 molecule is activated by interacting with 2-cyanopyridine to form a five-membered ring intermediate **I**. Subsequently, activated GL molecule makes a nucleophilic attack to the carbonyl carbon atom of the intermediate **I** to form intermediate **II**, and then the oxygen atom of the second O-H bond of GL makes an intramolecular nucleophilic attack on carbonyl carbon to give GC. Meanwhile, 2-cyanopyridine is transformed to 2-picolinamide. It is indicated that during the reaction, 2-cyanopyridine acts not only as a dehydrant, but also as a promoter for CO_2 activation.

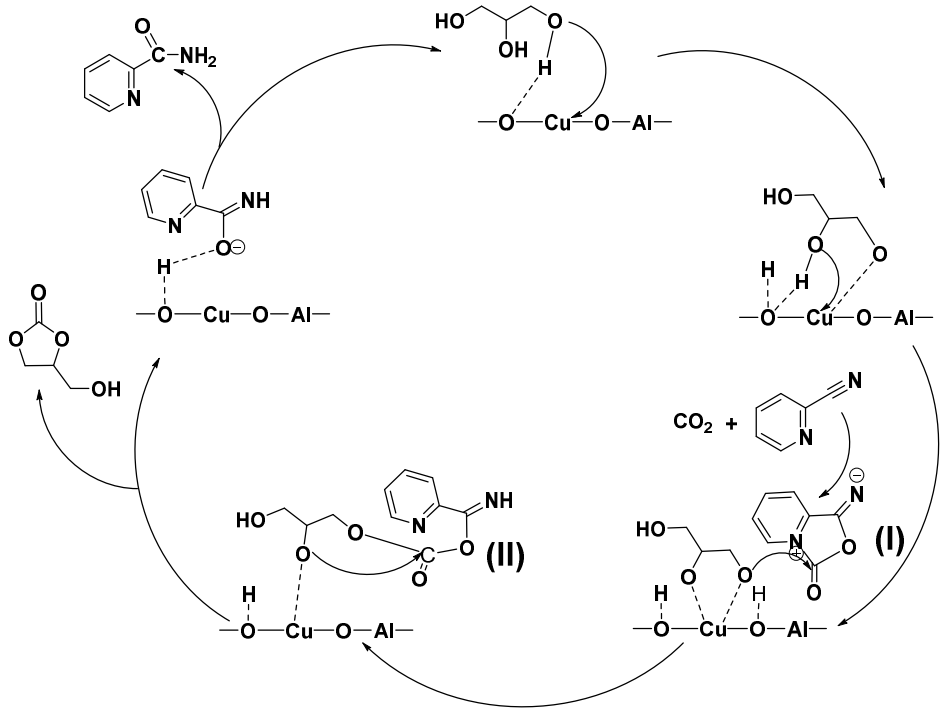

Scheme 3. The proposed reaction mechanism for the synthesis of GC from GL and CO_2 over CuO/Al_2O_3(30%, 700)

2.7. Comparison of the catalytic activity between different catalysts

Table 4. Comparison of catalytic activity of CuO/Al_2O_3(30%, 700) with the other catalysts for GC synthesis from GL and CO_2 [a]

Catalysts	T(°C)	Time(h)	P(MPa)	Cat.(wt%)	Dehydrant	X_{GL}(%)	Y_{GC}(%)	TOF[b]	Ref.
CeO_2	150	5	4	186.8	2-cyanopyride	-	78.9	0.92	[18]
$La_2O_2CO_3$–ZnO	170	12	4	5	acetonitrile	30.3	14.3	2.59	[31]
CHT-Cl	170	12	4	3.0	acetonitrile	35.5	16.7	4.97	[30]
ZnY	180	3	10	2.0	no	-	5.8	10.58	[24]
Cu/MCM-41	150	3	7	1.7	acetonitrile	18.7	1.8	3.81	[29]
CeO_2-nanopolyhedra	170	12	10	7.4	2-cyanopyride	35.5	14.2	1.74	[35]
ZnO	180	12	15	0.6	no	-	8.1	11.35	[25]
$Co(OAc)_2$	180	6	2	2.5	acetonitrile	36.7	4.6	3.33	[48]
$ZnWO_4$-ZnO	150	6	5	54.4	no	-	6.5	0.22	[23]
CuO/Al_2O_3(30%, 700)	150	5	4	43.6	2-cyanopyride	41.3	17.5	0.87	This work

[a] T: reaction temperature; Time: reaction time; P: reaction pressure of CO_2; Cat.: catalyst amount based on GL weight.

[b] TOF= mol of GC produced/(weight of catalyst · reaction time) (mmol/gcat·h).

Preprints (www.preprints.org) | NOT PEER-REVIEWED | Posted: 25 April 2023 doi:10.20944/preprints202304.0872.v1

The comparison of the catalytic activity of CuO/Al_2O_3(30%, 700) with the other catalysts for GC synthesis from GL and CO_2 is illustrated in Table 4. Although the different reaction conditions were used for these catalysts, these reaction conditions should be the optimized one for each catalyst. So, the catalytic activity of these catalysts can be compared by using the GC yields and TOFs at these optimal conditions. It is observed that due to the presence of dehydrant, the catalysts, such as CeO_2, $La_2O_2CO_3$–ZnO, CHT-Cl, CeO_2-nanopolyhedra, and CuO/Al_2O_3(30%, 700) show a higher GC yield than 14.0%. In contrary, the other catalysts, ZnY, ZnO, and $ZnWO_4$-ZnO give a lower GC yield than 9.0% for the dehydrant was not used during the reaction. It indicates that the dehydrant is very significant for the reaction of GL with CO_2. Among these catalysts, the activity of CuO/Al_2O_3(30%, 700) is only lower than that of CeO_2. However, CuO/Al_2O_3(30%, 700) has the remarkably lower catalyst amount than CeO_2. The higher catalytic activity of CuO/Al_2O_3(30%, 700) is ascribed to the synergistic effect of the catalyst and 2-cyanopyridine that the former has higher activation ability for GL and the latter acts as a promoter for CO_2 activation. The above results suggest that CuO/Al_2O_3(30%, 700) not only has higher catalytic activity and stability, but also has simple prepared process and cheap cost and thereby, it may be as a good alternative catalyst for the industrial production of GC from GL and CO_2.

3. Materials and Methods

3.1. Chemicals

Copper nitrate [$(Cu(NO_3)_2{\cdot}3H_2O$] (99% purity), activated alumina (Al_2O_3), silicon dioxide (SiO_2), activated carbone (AC), graphite, GL (99% purity), and methanol (99.5% purity) were bought from Sinopharm Chemical Reagent Co. Ltd., Beijing, China. 2-cyanopyridine (98% purity), tetraethylene glycol (99% purity), and 2-picolinamide (>98% purity) were purchased from Aladdin Industrial Corporation, Shanghai, China. Carbon dioxide (99.9% purity) was supplied by Wuhan Minghui Gas Technology Co. Ltd., Wuhan, China. GC (Tokyo Chemical Industry Co., Ltd., Tokyo, Japan) was of over 90% purity. N, N-dimethyl formamide (DMF) (99.5% purity) was purchased from Chinasun Speciality Products Co. Ltd., Jiangsu, China. All these chemicals were used without further purification.

3.2. Supported CuO-based nanoparticle catalyst preparation

The Al_2O_3, SiO_2, AC, graphene oxide (GO), and graphene (GE) were used as supports to prepare the supported CuO-based nanoparticle catalysts. The CuO/Al_2O_3 catalysts were prepared by the impregnation method using aqueous solution of $Cu(NO_3)_2{\cdot}3H_2O$ and activated alumina powder. Firstly, the activated alumina powder was dried under vacuum at 60 °C for 2 h to remove physisorbed water. Then, a certain amount of activated alumina (such as 7 g) was mixed with an aqueous solution of $Cu(NO_3)_2{\cdot}3H_2O$ (for example, 100 mL and the amount of $Cu(NO_3)_2{\cdot}3H_2O$ of 9.08g) in a glass flask. After strring for 15 min, the mixture was set for 24 h at room temperature and then dried at 100 °C for 1 h to remove water through evaporation. Subsequently, the solid mixture was grinded and sieved using the standard sieve with 100 mesh. The obtained solid powder was calcined at specified temperature (for example, 700 °C) for 5 h under static air. A heating ramp of 5 °C/min was employed in this step. Finally, the obtained catalyst was used in the reaction of GL and CO_2. All the prepared catalysts are denoted as CuO/Al_2O_3(n%, m), where n% is the weight percentage of CuO loaded on Al_2O_3 and m is the calcination temperature. The CuO/SiO_2(30%, 500) catalyst and CuO/AC(30%, 500) were prepared by the same method with CuO/Al_2O_3(30%, 500) using SiO_2 and AC as supports instead of Al_2O_3, respectively.

CuO/GO(30%, 500) was prepared by the procedure shown below. Firstly, the GO was obtained by the modified Hummers method. Briefly, 100 mL of the concentrated H_2SO_4 and 10 mL of the concentrated H_3PO_4 were poured into a beaker, and then, 2 g of graphite was added. The beaker was put in an ultrasonic cleaner for 1 h at 20 °C and 200 W. Subsequently, 0.75 g of $KMnO_4$ was added into the beaker, which was further treated by ultrasonic for another 2 h. Afterwards, the additional 3 g of $KMnO_4$ was added and the solution was stirred at 60 °C for 3 h. Then, the mixture was poured

Preprints (www.preprints.org) | NOT PEER-REVIEWED | Posted: 25 April 2023 doi:10.20944/preprints202304.0872.v1

into a large beaker with 190 mL of ice water, and then, 7.5 mL of H_2O_2 was added to give the graphite oxide. The sample was washed by centrifugation to be neutral and treated by ultrasonic dispersion at 200 W for 1h, and then, dried at 60 °C to give GO. The CuO/GO(30%, 500) was prepared by the same procedure with CuO/Al_2O_3(30%, 500) using GO as the support instead of Al_2O_3.

CuO/GE(30%, 500) was obtained by the following method: firstly, the GE was fabricated via a thermal exfoliation method. During the process, the dried GO was thermally exfoliated at 300 °C for 3 min in air and subsequently the sample was further treated at 900 °C for 3 h in air to give GE. The CuO/GE(30%, 500) was prepared by the same procedure with CuO/Al_2O_3(30%, 500) using GE as the support instead of Al_2O_3.

3.3. Catalyst characterization

X-ray diffraction (XRD) patterns of the catalysts were measured on a X'Pert PRO using Cu Kα radiation at 30 kV and 15 mA, over a 2θ range of 5° ~ 90° with a step size of 0.0167° at a scanning speed of 8 min^{-1}. A Bruker VERTEX 70 FT-IR spectrometer was used to obtain the FT-IR spectra of samples using KBr pellet technique, with 2 cm^{-1} resolution over the wavenumber range 4000-400 cm^{-1}. The morphology of the particles was observed by use of a scanning electron microscope (SEM, TESCAN VEGA3) with 20.0 kV of an accelerating voltage. Nitrogen adsorption-desorption isotherms were determined by a volumetric adsorption apparatus (Micromeritics ASAP 2420) at 77 K. The surface areas of samples were calculated by using the Brunauer-Emmett-Teller (BET) method. The pore volume was given at p/p0 =0.99. The pore size distribution was calculated by the Barrett-Joyner-Halenda (BJH) method.

The basicity studies of the prepared catalysts were conducted with temperature-programmed desorption of CO_2 as probe molecule (CO_2-TPD) using Huasi DAS-7000 apparatus equipped with thermal conductivity detector (TCD). The analysis was performed by heating 100 mg of the catalyst sample under a He flow from room temperature to 800 °C for 2 h (10 °C/min, 50 mL/min). Then, the temperature was decreased to 90 °C, and a flow of pure CO_2 (50 mL/min) was subsequently introduced into the reactor during 1 h. After the catalyst was swept with He for 1 h to remove the physisorbed CO_2 from catalyst surface, the TPD of CO_2 was carried out between 90 °C and 900 °C under a He flow (10 °C/min, 30 mL/min), and the detection of the desorbed CO_2 was performed by an on-line gas chromatograph provided with a TCD.

3.4. Reaction procedure

The tests of the catalytic activities of the metal oxide nanoparticle catalysts were carried out in a stainless-steel autoclave reactor of an inner volume of 250 mL equipped with thermostat, an electric heating jacket, pressure gauge, thermocouple, and agitator. After ascertaining the validity of the autoclave reactor, the typical procedure is as follows: 2.30 g of GL, 1.0 g of catalyst, 19.0 g of DMF, and 6.32 g of 2-cyanopyridine were put into the reactor together, and then, the reactor was sealed and purged with CO_2 for 3 times, and pressurized with CO_2 to 4 MPa. Subsequently, the reactor was heated to the reaction temperature (150 °C) and maintained for certain reaction time (5 h) under vigorous stirring (600 rpm). After reaction, the reactor was cooled to room temperature and depressurized. Then, all the product mixture was taken out from the autoclave reactor and the solid catalyst was separated by centrifugation from the liquid mixture. The collected catalyst was washed with methanol three times and then used in the recycle experiment. All of the liquid products were sampled for analysis. All the components were analyzed by the gas chromatograph (Fuli 9790-II) equipped with a flame ionization detector (FID) and a capillary column KB-WAX (30 m long, 0.25 mm i.d.). The internal standard method was used. The temperatures of the injector and the detector are 250 °C and 270 °C, respectively. The temperature of the column was programmed to have a 2-min initial hold at 70 °C, a 15 °C/min ramp from 70 °C to 250 °C and then a 15 min hold at 250 °C.

The conversion of GL, X_{GL}, the yield of GC, Y_{GC}, and the selectivity to GC, S_{GC} were calculated according to the following equations:

Preprints (www.preprints.org) | NOT PEER-REVIEWED | Posted: 25 April 2023 doi:10.20944/preprints202304.0872.v1

$$X_{GL} = \frac{n_{GL}^{in} - n_{GL}^{out}}{n_{GL}^{in}} \times 100\% \quad (1)$$

$$Y_{GC} = \frac{n_{GLC}^{out}}{n_{GL}^{in}} \times 100\% \quad (2)$$

$$S_{GC} = \frac{n_{GLC}^{out}}{n_{GL}^{in} - n_{GL}^{out}} \times 100\% \quad (3)$$

where n_{GL}^{in} is the initial mole number (mol) of GL while n_{GL}^{out} and n_{GLC}^{out} are the mole numbers (mol) of GL and GC in the residual reaction mixture after reaction, respectively.

5. Conclusions

To improve the conversion of GL to GC, supported CuO-based nanoparticles were prepared and used as catalyst in this transformation. CuO/Al_2O_3 shows excellent catalytic activity for the synthesis of GC from GL and CO_2. Both the calcination temperature and CuO loading amount exhibit significant effect on the catalytic activity of CuO/Al_2O_3 catalyst. A larger surface area and higher amount of basic sites are crucial for the reaction of GL with CO_2. FT-IR characterization clear shows that during the reaction, 2-cyanopyridine acts not only as a dehydrant, but also as a promoter to active the chemically inert CO_2. The GL conversion and GC yield can reach to 41.3% and 17.5%, respectively, under the CO_2 pressure of 4.0 MPa, 150 °C, 5 h over CuO/Al_2O_3(30%, 700) catalyst. This catalyst with a higher catalytic activity, stability, simple prepared process, and cheap cost may be used as an alternative component for the industrial process.

Funding: This research was funded by the Fundamental Research Funds for the Central Universities of China (2011QN117).

Acknowledgements: XRD and SEM analysis was performed in the Analytical and Testing Center, and FT-IR analysis was performed in the Experimental Teaching Center of Chemistry and Chemical Engineering, School of Chemistry and Chemical Engineering, Huazhong University of Science and Technology.

Author Contributions: All authors have read and agreed to the published version of the manuscript.

Conflicts of Interest: The authors declare no conflict of interest

References

1. Guedes, P.H.P.S.; Luz, R.F.; Cavalcante, R.M.; Young, A.F. Process simulation for technical and economic evaluation of acrolein and glycerol carbonate production from glycerol. Biomass Bioenerg. **2023**, 168, 106659.
2. Wang, H.; Lu, P. Liquid−liquid equilibria for the system dimethyl carbonate + methanol + glycerol in the temperature range of (303.15 to 333.15) K. J. Chem. Eng. Data **2012**, 57, 582-589.
3. Hu, K.; Wang, H.; Liu, Y.; Yang, C. KNO_3/CaO as cost-effective heterogeneous catalyst for the synthesis of glycerol carbonate from glycerol and dimethyl carbonate. J. Ind. Eng. Chem. **2015**, 28, 334-343.
4. Lu, P.; Wang, H.; Hu, K. Synthesis of glycerol carbonate from glycerol and dimethyl carbonate over the extruded CaO-based catalyst. Chem. Eng. J. **2013**, 228, 147-154.
5. Ye, X.; Wang, W.; Zhao, X.; Wen, T.; Li, Y.; Ma, Z.; Wen, L.; Ye, J.; Wang, Y. The role of the $KCaF_3$ crystalline phase on the activity of KF/CaO biodiesel synthesis catalyst. Catal. Commun. **2018**, 116, 72-75.
6. Das, B.; Mohanty, K. A green and facile production of catalysts from waste red mud for the one-pot synthesis of glycerol carbonate from glycerol. J. Environ. Chem. Eng. **2019**, 7, 102888.
7. Ambat, I.; Srivastava, V.; Sillanpä, M. Recent advancement in biodiesel production methodologies using various feedstock: a review. Renew. Sustain. Energy Rev. **2018**, 90, 356-369.
8. Li, W.; Sreerangappa, R.; Estager, J.; Monbaliu, J.C.M.; Debecker, D.P.; Luis, P. Application of pervaporation in the bio-production of glycerol carbonate. Chemical Engineering & Processing: Process Intensification **2018**, 132, 127-136.

9. Singh, D.; Sharma, D.; Soni, S. L.; Sharma, S.; Sharma, P.K.; Jhalani, A. A review on feedstocks, production processes, and yield for different generations of biodiesel. Fuel **2020**, 262, 116553.
10. Yu, J.; Wang, K.; Shao, S.; Li, W.; Du, S.; Chen, X.; Chao, Cong.; Fan. X. Effect of ionic radius and valence state of alkali and alkaline earth metals on promoting the catalytic performance of La2O3 catalysts for glycerol carbonate production. Chem. Eng. J. **2023**, 458, 141486.
11. Esteban, J.; Vorholt, A.J. Obtaining glycerol carbonate and glycols using thermomorphic systems based on glycerol and cyclic organic carbonates: Kinetic studies. J. Ind. Eng. Chem. **2018**, 63, 124-132.
12. Li, Y.; Liu, J.; He, D. Catalytic synthesis of glycerol carbonate from biomass-based glycerol and dimethyl carbonate over Li-La_2O_3 catalysts. Appl. Catal. A: Gen. **2018**, 564, 234-242.
13. Wan, Y.; Lei, Y.; Lan, G.; Liu, D.; Li, G.; Bai, R. Synthesis of glycerol carbonate from glycerol and dimethyl carbonate over DABCO embedded porous organic polymer as a bifunctional and robust catalyst. Appl. Catal. A: Gen. **2018**, 562, 267-275.
14. Costanzo, P.; Calandruccio, C.; Di Gioia, M.L.; Nardi, M.; Oliverio, M.; Procopio, A. First multicomponent reaction exploiting glycerol carbonate synthesis. J. Cleaner Prod. **2018**, 202, 504-509.
15. Fernandes, G.P.; Yadav, G.D. Selective glycerolysis of urea to glycerol carbonate using combustion synthesized magnesium oxide as catalyst. Catal. Today **2018**, 309, 153-160.
16. Wang, H.; Liu, T.; Jiang, C.; Wang Y.; Ma, J. Synthesis of glycidol and glycerol carbonate from glycerol and dimethyl carbonate using deep-eutectic solvent as a catalyst. Chem. Eng. J. **2022**, 442, 136196
17. Das, A.; Shi, D.; Halder, G.; Rokhum, S.L. Microwave-assisted synthesis of glycerol carbonate by transesterification of glycerol using Mangifera indica peel calcined ash as catalyst. Fuel **2022**, 330, 125511.
18. Liu, J.; Li, Y.; Zhang, J.; He, D. Glycerol carbonylation with CO_2 to glycerol carbonate over CeO_2 catalyst and the influence of CeO_2 preparation methods and reaction parameters. Appl. Catal. A: Gen. **2016,** 513, 9-18.
19. Zhang, J.; He, D. Surface properties of Cu/La_2O_3 and its catalytic performance in the synthesis of glycerol carbonate and monoacetin from glycerol and carbon dioxide. J. Colloid Interface Sci. **2014**, 419, 31-38.
20. Elhaj, E.; Wang, H.; Gu, Y. Functionalized quaternary ammonium salt ionic liquids (FQAILs) as an economic and efficient catalyst for synthesis of glycerol carbonate from glycerol and dimethyl carbonate. Molecular Catalysis **2019**, 468, 19-28.
21. George, J.; Patel, Y.; Pillai, S.M.; Munshi, P. Methanol assisted selective formation of 1,2-glycerol carbonate from glycerol and carbon dioxide using $^{n}Bu_2SnO$ as a catalyst. J. Mol. Catal. A: Chem. **2009**, 304, 1-7.
22. Liu, J.; Li, Y.; Liu, H.; He, D. Transformation of CO_2 and glycerol to glycerol carbonate over CeO_2-ZrO_2 solid solution—effect of Zr doping. Biomass and Bioenergy **2018**, 118, 74-83.
23. J. Liu, D. He, Transformation of CO_2 with glycerol to glycerol carbonate by a novel $ZnWO_4$-ZnO catalyst. Journal of CO_2 Utilization **2018**, 26, 370-379.
24. Ozorio, L.P.; Pianzolli, R.; Machado, L.C.; Miranda, J.L.; Turci, C.C.; Guerra, A.C.O.; Souza-Aguiar, E.F.; Mota, C.J.A. Metal-impregnated zeolite Y as efficient catalyst for the direct carbonation of glycerol with CO_2. Appl. Catal. A: Gen. **2015**, 504, 187-191.
25. Ozorio, L.P.; Mota, C.J.A. Direct carbonation of glycerol with CO_2 catalyzed by metal oxides. ChemPhysChem **2017**, 18; 3260-3265.
26. Li, J.; Wang, T. Chemical equilibrium of glycerol carbonate synthesis from glycerol. J. Chem. Thermodynamics **2011**, 43, 731-736.
27. Vieville, C.; Yoo, J.W.; Pelet, S.; Mouloungui, Z. Synthesis of glycerol carbonate by direct carbonatation of glycerol in supercritical CO_2 in the presence of zeolites and ion exchange resins. Catalysis Letters **1998**, 56, 245-247.
28. Dibenedetto, A.; Angelini, A.; Aresta, M.; Ethiraj, J.; Fragale, C.; Nocito, F. Converting wastes into added value products: from glycerol to glycerol carbonate, glycidol and epichlorohydrin using environmentally friendly synthetic routes. Tetrahedron **2011**, 67, 1308-1313.
29. Aresta, M.; Dibenedetto, A.; Nocito, F.; Pastore, C. A study on the carboxylation of glycerol to glycerol carbonate with carbon dioxide: the role of the catalyst, solvent and reaction conditions. J. Mol. Catal. A: Chem. **2006**, 257, 149-153.
30. Zhang, J.; He, D. Synthesis of glycerol carbonate and monoacetin from glycerol and carbon dioxide over Cu catalysts: the role of supports. J. Chem. Technol. Biotechnol. **2015**, 90, 1077-1085.
31. Li, H.; Xin, C.; Jiao, X.; Zhao, N.; Xiao, F.; Li, L.; Wei, W.; Sun, Y. Direct carbonylation of glycerol with CO_2 to glycerol carbonate over Zn/Al/La/X (X=F, Cl, Br) catalysts: the influence of the interlayer anion. J. Mol. Catal. A: Chem. **2015**, 402, 71-78.

32. Li, H.; Gao, D.; Gao, P.; Wang, F.; Zhao, N.; Xiao, F.; Wei, W.; Sun, Y. The synthesis of glycerol carbonate from glycerol and CO_2 over $La_2O_2CO_3$–ZnO catalysts. Catal. Sci. Technol. **2013**, 3, 2801-2809.
33. Park, C.; Nguyen-Phu, H.; Shin, E.W. Glycerol carbonate with CO_2 and $La_2O_2CO_3$/ZnO catalysts prepared by two different methods: preferred reaction route depending on crystalline structure. Molecular Catalysis, **2017**, 435, 99-109.
34. Ma, J.; Song, J.; Liu, H.; Liu, J.; Zhang, Z.; Jiang, T.; Fan, H.; Han, B. One-pot conversion of CO_2 and glycerol to value-added products using propylene oxide as the coupling agent. Green Chem. **2012**, 14, 1743-1748.
35. Su, X.; Lin, W.; Cheng, H.; Zhang, C.; Wang, Y.; Yu, X.; Wu, Z.; Zhao, F. Metal-free catalytic conversion of CO_2 and glycerol to glycerol carbonate. Green Chem. **2017**, 19, 1775-1781.
36. Lv, Y.; Zhang, H.; Yao, X.; Dong, L.; Chen, Y. Investigation of the physicochemical properties of CuO/Sm_2O_3/γ-Al_2O_3 catalysts and their activity for NO removal by CO. J. Mol. Catal. A: Chem. **2016**, 420, 34-44.
37. Ajamein, H.; Haghighi, M.; Shokrani, R.; Abdollahifar, M. On the solution combustion synthesis of copper based nanocatalysts for steam methanol reforming: Effect of precursor, ultrasound irradiation and urea/nitrate ratio. J. Mol. Catal. A: Chem. **2016**, 421, 222-234.
38. Sodeifian, G.; Behnood, R. Application of microwave irradiation in preparation and characterization of CuO/Al_2O_3 nanocomposite for removing MB dye from aqueous solution. Journal of Photochemistry and Photobiology A: Chemistry **2017**, 342, 25–34.
39. Ha, J.; Ryu, H.; Lee, W.; Bae, J. Efficient photoelectrochemical water splitting using CuO nanorod/Al_2O_3 heterostructure photoelectrodes with different Al layer thicknesses. Physica B **2017**, 519, 95–101.
40. Ajamein, H.; Haghighi, M.; Alaei, S. Influence of propylene glycol/nitrates ratio on microwave-assisted combustion synthesis of CuO-ZnO-Al_2O_3 nanocatalyst: structural and catalytic properties toward hydrogen production from methanol. Materials Research Bulletin **2018**, 102, 142–152.
41. Luo, M.; Fang, P.; He, M.; Xie, Y. In situ XRD, Raman, and TPR studies of CuO/Al_2O_3 catalysts for CO oxidation. J. Mol. Catal. A: Chem. **2005**, 239, 243-248.
42. Shaheen, W.M. Thermal solid-solid interaction and catalytic properties of CuO/Al_2O_3 system treated with ZnO and MoO_3. Thermochimica Acta **2002**, 385, 105-116.
43. Salavati-Niasari, M.; Davar, F.; Farhadi, M. Synthesis and characterization of spinel-type $CuAl_2O_4$ nanocrystalline by modified sol–gel method. J. Sol-Gel Sci. Technol. **2009**, 51, 48–52.
44. Lv, W.; Liu, B.; Qiu, Q.; Wang, F.; Luo, Z.; Zhang, P.; Wei, S. Synthesis, characterization and photocatalytic properties of spinel $CuAl_2O_4$ nanoparticles by a sonochemical method. Journal of Alloys and Compounds **2009**, 479, 480–483.
45. Tomishige, K.; Ikeda, Y.; Sakaihori, T.; Fujimoto, K. Catalytic properties and structure of zirconia catalysts for direct synthesis of dimethyl carbonate from methanol and carbon dioxide. J. Catal. **2000**, 192, 355-362.
46. Ochoa-Gómez, J.R.; Gómez-Jiménez-Aberasturi, O.; Maestro-Madurga, B.; Pesquera-Rodríguez, A.; Ramírez-López, C.; Lorenzo-Ibarreta, L.; Torrecilla-Soria, J.; Villarán-Velasco, M.C. Synthesis of glycerol carbonate from glycerol and dimethyl carbonate by transesterification: Catalyst screening and reaction optimization. Appl. Catal. A: Gen. **2009**, 366, 315-324.
47. Ishak, Z.I.; Sairi, N.A.; Alias, Y.; Aroua, M.K.T.; R. Yusoff, Production of glycerol carbonate from glycerol with aid of ionic liquid as catalyst, Chem. Eng. J. **2016,** 297, 128-138.
48. Liu, Y. Synthesis of glycerol carbonate from glycerol and carbon dioxide over cobalt acetate catalyst. Speciality Petrochemicals **2014**, 31, 25-27. (in chinese)